ground water

Effects of Gas Generation and Precipitates on Performance of Fe° PRBs

by Yousheng Zhang[1] and Robert W. Gillham[2]

Abstract

Long-term reactivity and permeability are critical factors in the performance of granular iron permeable reactive barriers (PRBs). Thus it is a topic of great practical importance, as well as scientific interest. In this study, four types of source solutions (distilled H_2O, 10 mg/L TCE, 300 mg/L $CaCO_3$, and 10 mg/L TCE + 300 mg/L $CaCO_3$) were supplied to four columns containing a commercial granular iron material. In all four columns, gases accumulated to ~ 10% of the initial porosity and resulted in declines in permeability of ~ 50% to 80%. In the columns receiving $CaCO_3$, carbonate precipitates accumulated to ~ 7% of the initial porosity, with no apparent decline in permeability. The data indicate that precipitates formed initially at the influent ends of the columns, reducing the reactivity of the iron in this region. As a consequence of the reduced reactivity, calcium and bicarbonate migrated further into the column, to precipitate in a region where the reactivity remained high. Thus precipitation occurred as a moving front through the columns. The results suggest improved methods for PRB design and rehabilitation, and also suggest improvements that are needed in the mathematical models developed for predicting long-term performance.

Introduction

The use of granular iron for in situ treatment of ground water containing halocarbons is promoted as a cost-effective alternative to conventional treatment methods. However, because the capital cost of installing a granular iron permeable reactive barrier (PRB) can be substantial, in most situations, the cost benefit must be realized through greatly reduced operating and maintenance costs. A significant requirement in meeting this criterion is that the granular iron within the PRB perform consistently and effectively over long periods of time.

The initial field demonstration of the technology showed no decline in performance over the five-year duration of the study (O'Hannesin and Gillham 1998), and more recent studies indicate that after 10 years, there has been little or no decline in the reactivity of the iron (Reynolds 2002). Furthermore, the evidence suggests that the first installation at an industrial site, in 1994, continues to perform effectively (Sorel et al. 2003). Though the empirical evidence is encouraging, and is becoming more convincing as the period of record lengthens, there continues to be an uncertain basis for predicting performance well into the future. The primary issues, as suggested in Gillham and O'Hannesin (1994) and Gillham (1999), concern the longevity of the iron, the activity of the iron surfaces, and the effects that precipitates may have on both reactivity and permeability.

Following Gillham and O'Hannesin (1994) and Matheson and Tratnyek (1994), the net effect of the corrosion of iron by water and by chlorinated solvents is the production of H_2; the release of Fe^{2+} to solution; an increase in pH, often to values in excess of 10; and a decrease in Eh to strongly reducing conditions. If produced in sufficient quantities, H_2 may form a separate gas phase with the potential to reduce hydraulic conductivity and thus have an adverse effect on performance. For example, gas accumulations in granular iron of 10% to 15% (Mackenzie et al. 1999) and 20% (Repta 2001) of the initial porosity have been reported. In addition to reduced permeability, entrapped hydrogen or other gases could reduce reaction rates by reducing the area of iron exposed to the solution phase.

The effect of a wide range of inorganic constituents of ground water on the reactivity of granular iron is an active

[1]SEACOR Environmental Inc., 201-6200 Dixie Rd., Mississauga, Ontario, L5T 2E1
[2]Corresponding author: Department of Earth Sciences, University of Waterloo, Waterloo, Ontario N2L 3G1, Canada; (519) 888–4658; fax: (519) 746–1829; rwgillha@sciborg.uwaterloo.ca
Received March 2003, accepted September 2003.

topic of research. Two recent and notable publications based on long-term laboratory tests include Farrel et al. (2000) and Klausen et al. (2003). The reason for observed declines in reactivity is generally inferred to be the formation of surface films, and in many cases films have been identified and characterized through surface analyses. Examples of mineral phases that have been identified on iron surfaces include iron hydroxide (Bonin et al. 2000), magnetite (Bonin et al. 2000), aragonite (Phillips et al. 2000), siderite (Agrawal et al. 2002), ferric hydroxide (Mackenzie et al. 1999), manganese oxyhydroxide (Okwi et al. in press), chromium oxyhrdoxides (Blowes et al. 1997), silica complexes (Klausen et al. 2003), and carbonate-containing green rust (Bonin et al. 2000).

Bicarbonate is present in most ground waters, and frequently at concentrations in excess of 100 mg/L. At the elevated pH values within a granular iron PRB, bicarbonate is converted to carbonate, with the potential to form several precipitates, depending upon the chemical characteristics of the water, but most commonly precipitates of iron, calcium, and magnesium. Indeed, the precipitate identified most commonly and in greatest abundance at field sites is calcium carbonate (Gallant and Myller 1997; McMahon et al. 1999; Vogan et al. 1999). In particular, Vogan et al. (1999) showed calcium carbonate accumulations of up to 6% of the initial porosity near the upgradient face of a PRB, and based on the results of laboratory tests, Fort (2000) estimated porosity losses of 2% to 5% annually. There is, however, little information on the pattern of precipitate formation over time. In particular, though precipitation of calcium carbonate is commonly observed to occur initially at the influent end of laboratory columns, or the influent face of PRBs, it is uncertain if the precipitates will accumulate in quantities such that the upgradient region becomes essentially impermeable or if the precipitates will occur progressively along the column (through the PRB). Furthermore, though short-term laboratory experiments suggest that calcium carbonate minerals have a minor effect on the reactivity of the iron, the long-term effects of progressive precipitation remain uncertain.

This study was undertaken to determine the effects of entrapped gas and calcium carbonate mineral precipitates on porosity and hydraulic conductivity of granular iron. A particular objective was to determine the pattern of precipitate formation and to relate this pattern to the reactivity of the iron. The study involved long-term monitoring of laboratory columns.

Materials and Methods

Four plexiglass columns measuring 3.81 cm I.D. and 10 cm in length were each fitted with three sampling ports located at 2.5, 5.0, and 7.5 cm from the influent end. All of the columns were packed dry with, as received, commercial granular iron obtained from Master Builders of Cleveland, Ohio. The grain size was within the range of 18 to 60 mesh and the BET surface area was 1.5 m^2/g. Each column received a different solution: (1) distilled water, (2) 10 mg/L trichloroethene (TCE) in distilled water, (3) 300 mg/L $CaCO_3$ in distilled water, and (4) 10 mg/L TCE + 300 mg/L $CaCO_3$ in distilled water. These columns will be referred to as water, TCE, $CaCO_3$, and TCE + $CaCO_3$, respectively. The temperature in the laboratory was 22° ±3°C.

To prepare the carbonate solution, 3 g of $CaCO_3$ was added to a 15 L carbuoy containing 10 L of distilled water. The solution was then bubbled with CO_2 gas to dissolve the $CaCO_3$. All the source solutions in this study were deoxygenated by purging with O_2-free N_2 for two hours. The O_2 concentration was reduced to below 0.2 mg/L and the pH increased to 6.8 ± 0.2 as the CO_2 was purged from the solution. Purging of the TCE and TCE + $CaCO_3$ solutions was conducted prior to the addition of TCE. The source solutions were stored in 15 L glass carbuoys, and pumped to the bottom (influent) end of the respective columns (Figure 1). To avoid oxygen contamination, with the exception of a 15 cm length of Viton tubing that passed through the pump, stainless steel tubing was used to connect the source bottles to the columns. As a further precaution, mylar balloons filled with oxygen-free N_2 gas were used to supply the headspace as the solution level declined in the source bottles. For the solutions containing TCE, the N_2 gas from the balloons first passed through a bottle filled with a solution identical to the source solution to raise the TCE concentration in the gas before it passed into the source bottles.

Plastic tubing connected to a "T" valve near the inlet to each column was used as a manometer to monitor the hydraulic head at the inlet. The hydraulic gradient across the column was calculated using the hydraulic head at the bottom of the column, as reflected in the manometer reading, and the hydraulic head at the top of the column, as determined from the elevation of the drip point entering the waste container. Hydraulic conductivity was then calculated from the gradient and the solution flux, using the Darcy equation. The effluent from the column passed through a sealed glass tube to trap the gases, before emptying into the waste container. The gas volume was measured periodically in order to calculate rates of gas production. Periodically, the columns were disconnected and weighed, and the effluent volumes were recorded.

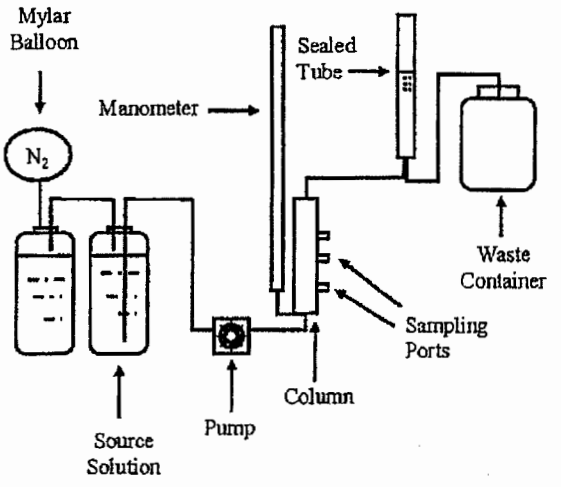

Figure 1. Schematic of the column apparatus.

The respective source solutions were introduced at a flow rate of approximately 0.44 mL/min using an Ismatec Multichannel Cartridge Pump (Model 78001–02). Flow velocity varied as a consequence of changes in water-filled porosity, but the initial values were close to 1.1×10^{-3} cm/s. Thus the time to displace one pore volume (PV) of solution was approximately 2.4 hr for all four columns. The initial porosity values were determined knowing the volume of each column, the mass of iron added to each column, and the particle density of the iron (6.56 g/cm^3).

The concentrations of oxygen and TCE were monitored in the source bottles. In the event that the TCE concentration dropped below 9 mg/L, a measured amount of TCE was added to maintain the concentration near 10 mg/L. In addition, on occasion, the source solution was replaced immediately if oxygen levels > 0.2 mg/L were detected.

Samples (8 mL) taken from the inlet, outlet, and the three sampling ports were collected and analysed weekly for TCE and possible degradation products. The TCE sample was prepared for analysis by adding 1 mL of sample to 2 mL of pentane in a 5 mL bottle. Samples used to analyse for degradation products [dichloroethene (DCE) isomers and vinyl chloride (VC)] were prepared by adding 4 mL of sample to a 10 mL hypovial for head-space analysis. All samples were shaken for an equilibration period of 15 min prior to analysis. A Hewlett-Packard 5890 gas chromatograph equipped with an ECD detector and autosampler was used for the analysis of TCE and a Hewlett Packard GC with a HNu PID detector and autosampler was used for DCE and VC analyses. Alkalinity, pH, Eh, and calcium were determined using the remaining solution. The pH and Eh were measured using a Markson pH/temperature meter (Model 90), alkalinity was determined by titration, and Ca by atomic absorption. The columns were sectioned at the conclusion of the experiment and calcium carbonate precipitates in subsamples of the solids were quantified using a modified Bundy and Bremner (1972) method.

Results and Discussion

Effects of Hydrogen Production on Column Porosity and Hydraulic Conductivity

Figure 2 shows the relative weight of each column over time, where relative weight was calculated as the measured weight of a column minus the initial weight of the apparatus without iron, divided by the initial total weight (including iron and water) minus the initial mass of apparatus without iron. Considering an iron corrosion rate by water of 0.4 mmole/kg Fe°/d (Reardon 1995) and complete dechlorination of TCE, the maximum consumption of Fe° was calculated to be 0.43 g/d. Further assuming that the oxidized iron forms Fe_3O_4 (Ritter et al. 2002), iron reactions could result in a net increase in the weight of a column of 0.14 g/d. This would give a change in relative weight of $\sim +3 \times 10^{-4}$ and was therefore considered inconsequential. Thus, changes in relative weight were considered to reflect gas accumulation in the column, as well as precipitate formation.

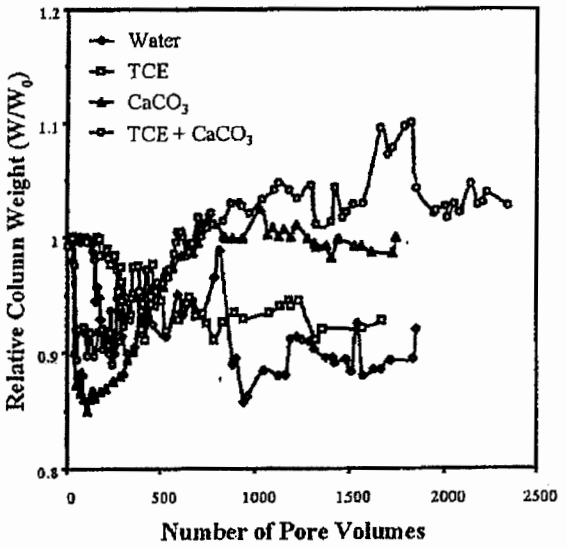

Figure 2. Changes in relative column weight over time.

The relative weight of all columns remained reasonably steady for the first 30 PV, after which gas bubbles could be seen through the Plexiglas® walls of the columns receiving the $CaCO_3$ and TCE + $CaCO_3$ solutions. The weights of these columns began to decline quickly and gas bubbles began to appear in the effluent within a further 50 PV. Similar changes were observed in the water and TCE columns, though the weight decline was not evident until ~ 150 PV and the decline was slower. For all columns, the decline in weight was considered to be caused by the accumulation of the gas phase in the pore structure of the granular iron. Though analyses were not performed, the majority of the gas is believed to have been H_2, formed as a consequence of iron corrosion. The more rapid decline in the columns receiving carbonate solutions suggests these solutions to be more corrosive than the distilled water and distilled + TCE solutions. This is consistent with the work of Dahmke et al. (2000), Bonin et al. (2000), and Agrawal et al. (2002), who showed that iron corrosion with water was enhanced in the presence of bicarbonate.

Using the influent and effluent alkalinity values, if all the bicarbonate lost during the first 50 PV precipitated as $CaCO_3$, it would represent an increase in relative weight of only 0.01. Thus, the decline in weight over this period is a reasonable measure of the volume of entrapped gas. The initial water-filled porosity and the water-filled porosity at gas breakthrough were used to calculate the maximum percentage of the initial porosity that became gas filled (Table 1). The values range from 6.3% to 13.8%; however, because of the scatter in the data (Figure 2), it is not possible to attach any significance to the variation in terms of the different treatments, and a uniform porosity loss of ~ 10% is suggested as reasonable. The scatter in Figure 2 is undoubtedly a consequence of unsteady gas distributions in the columns as well as the occurrence of periodic releases of gas to the effluent. Similar erratic behaviour in columns

Table 1
Porosity and Hydraulic Conductivity of Columns Measured at Early Time (Initial) and Following Gas Breakthrough

Column	Water-Filled Porosity			Hydraulic Conductivity (cm/s)		
	Initial	After Gas Breakthrough	Loss (% of initial)	Initial ($\times 10^{-3}$)	After Gas Breakthrough ($\times 10^{-4}$)	Loss (% of initial)
Water	0.59	0.53	10.2	2.2	3.9	82.3
TCE	0.63	0.59	6.3	2.2	7.5	65.9
$CaCO_3$	0.58	0.52	10.3	1.1	5.0	54.5
TCE + $CaCO_3$	0.63	0.54	13.8	1.8	31.9	—

where a gas phase was produced is reported in Morrison et al. (1996) and Fryar and Schwartz (1998).

In the water and TCE columns, after gas breakthrough, the column weights remained relatively steady for the duration of the experiment. Thus, at least in the laboratory environment and on the time scale of the experiment (500 d), there was no evidence of recovery of the porosity initially lost to the entrapped gas. As discussed in a later section, the increasing weight in the columns receiving carbonate solutions is attributed to precipitate formation.

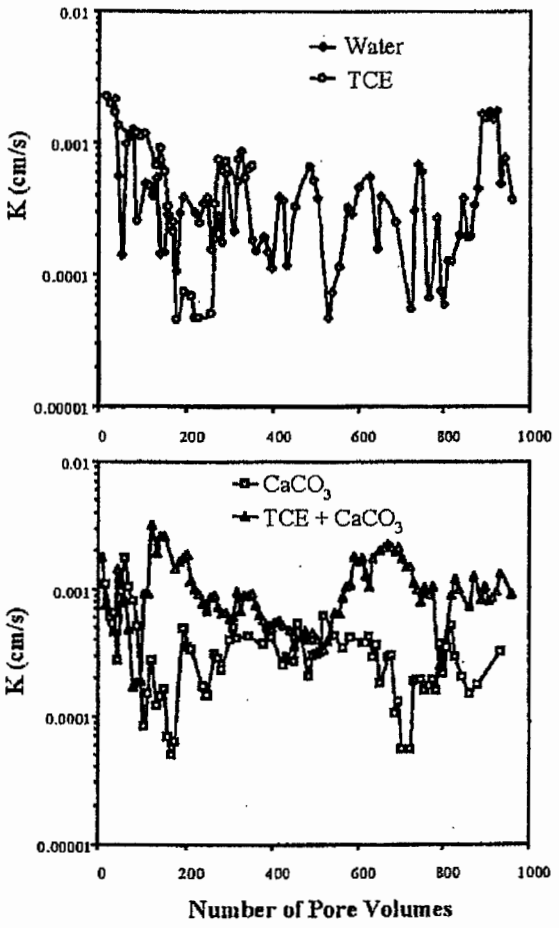

Figure 3. Changes in hydraulic conductivity, K, in the column over time: (a) columns that did not receive $CaCO_3$; (b) columns that received $CaCO_3$.

Because the trends appeared to be well established, hydraulic head measurements were terminated at ~ 950 PV in three of the columns. The TCE column was essentially a duplicate of the water column with respect to gas and precipitate production, and thus hydraulic head measurements in the TCE column were terminated after ~ 350 PV. Figure 3 shows the hydraulic conductivity of each column over time. As in Figure 2, the scatter in the data is believed to be largely a consequence of the periodic release of gas from the columns. Because the gas phase is non-wetting, it accumulates in the largest pores, and because the largest pores are the most effective in transmitting water, relatively small changes in the gas-filled porosity can have a large influence on the hydraulic conductivity, accentuating the scatter in Figure 3. The periodic occurrence of gas bubbles in the effluent lines would contribute further variation as a consequence of uncertainty in the hydraulic head at the effluent end of the columns. In spite of the uncertainty and the scatter in the data, the graphs of Figure 3 show trends that are worthy of discussion.

The greatest change in hydraulic conductivity occurred in the early stages of the experiment during the period of gas accumulation and gas breakthrough. All columns showed a decline in hydraulic conductivity in the range of about one order of magnitude or greater, followed by recovery once the gas broke through the columns. Thus, once the bubbling pressure of the porous medium was exceeded and the preferred pathways for gas migration were established, the hydraulic conductivity recovered to some degree.

Table 1 shows the measured value of the initial hydraulic conductivity, and the "recovered" value following gas breakthrough. The decline in hydraulic conductivity, as a consequence of gas entrapment, varied from 54% to 82%, though, because of the unexplained behavior (Figure 3), a value was not calculated for the TCE + $CaCO_3$ column.

Effects of Carbonate Precipitates on Porosity and Hydraulic Conductivity

The amount of carbonate precipitate formed in the respective columns was calculated in four ways: (1) from the change in weight of the columns over time, (2) from the difference over time in alkalinity between the influent and

effluent solutions, (3) from the difference over time in the calcium concentration between the influent and effluent solutions, and (4) from sectioning the columns at the end of the experiment and performing an acid digestion and titrating the resulting solution for alkalinity. As shown in Figure 2, following breakthrough of the gas phase, the columns receiving calcium carbonate solution showed a gradual increase in weight. This occurred over the period from ~ 250 to 800 PV in the case of the carbonate column, and 250 to ~ 1100 PV in the case of the TCE + $CaCO_3$ column. Consistent with the longer period of precipitation, there was a greater accumulation of precipitates in the TCE + $CaCO_3$ column than in the $CaCO_3$ column. The relatively constant mass beyond ~ 1000 PV suggests that precipitation occurred to some maximum level, beyond which the conditions were such that there was no further precipitation. Assuming calcite to be the primary precipitate, and using the increase in weight and a molar volume of 36.9 cm^3, the volume of precipitate formed in each column was determined, from which the percentage reduction of the initial porosity was calculated. The increase in weight, precipitate volume, and porosity loss are given in Table 2. As indicated, the porosity reduction was 6% for the $CaCO_3$ column and 7% for the TCE + $CaCO_3$ column. As noted in Mackenzie et al. (1999), using the molar volume to calculate the volume of precipitate does not take into account the loose structure of freshly precipitated mineral materials. While it may be reasonable to increase the volume of precipitate in proportion to its porosity, we could find no quantitative basis for performing this step. Thus the percent porosity loss, as included in Table 2, should be viewed as minimum values.

The influent and effluent bicarbonate and calcium concentrations were measured periodically over the course of the study. Treating calcium and bicarbonate independently, and assuming that each was consumed only as a consequence of precipitation of $CaCO_3$, Figure 4 shows the mass of $CaCO_3$ accumulation over time in the respective columns. It should first be noted, that with the exception of the $CaCO_3$ accumulation calculated using the decline in alkalinity across the $CaCO_3$ + TCE column, the two methods gave similar results, and results that were similar to those determined from measurements of column weight. In the absence of a reasonable explanation, we believe the results obtained from the decline in alkalinity in the $CaCO_3$ + TCE column to be anomalous. Similar to the results

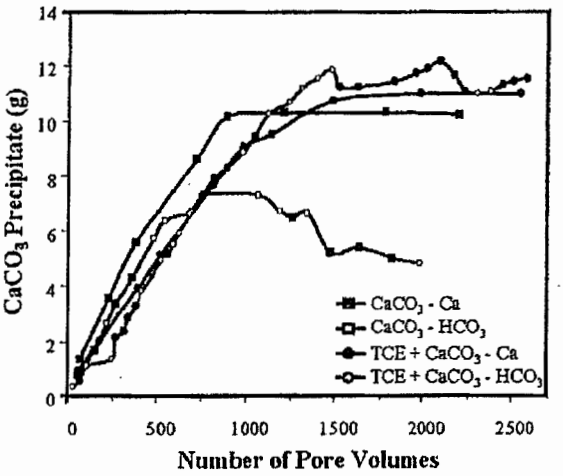

Figure 4. Accumulation of $CaCO_3$ in carbonate and TCE + carbonate columns calculated from changes in HCO_3^- and Ca^{2+} across the columns.

obtained from the weight measurements, the mass of $CaCO_3$ precipitate appeared to reach a maximum at ~ 800 PV in the $CaCO_3$ column and ~ 1300 PV in the $CaCO_3$ + TCE column, with no further precipitate accumulation to the end of the experiment. The mass of precipitate accumulation in each column, along with calculated precipitate volume and porosity loss, are included in Table 2.

At the conclusion of the study the two columns receiving carbonate solution were divided into three segments and analyzed for $CaCO_3$. The results are given in Table 3. This test does not show trends over time, but it does indicate similar amounts of $CaCO_3$ over the length of each column, and shows the total amount of precipitate in the two columns to be similar.

Referring to Table 2, the four methods of determination gave remarkably similar values for the mass of precipitate that accumulated in the two columns. The range for the $CaCO_3$ column was 9.9 to 10.6 g, and for the TCE + $CaCO_3$ column was 9.4 to 11.5 g. With respect to loss of initial porosity, the range was 6.0% to 6.3 % (average of 6.1%) for the $CaCO_3$ column and 6.2% to 7.6% (average of 7.0%) for the TCE + $CaCO_3$ column. Though the change in porosity values for the two columns were similar, the larger

Table 2
Mass and Volume of Calcium Carbonate Precipitate and Percent of Porosity Loss as Determined by Different Methods[a]

Column	Mass (g)				Volume (cm^3)				Porosity Loss (%)			
	M_1	M_2	M_3	M_4	M_1	M_2	M_3	M_4	M_1	M_2	M_3	M_4
$CaCO_3$	9.9	7.5[b]	10.3	10.6	3.7	2.8[b]	3.8	3.9	6.0	4.5[b]	6.1	6.3
TCE + $CaCO_3$	10.4	11.5	9.4	11.4	3.9	4.3	3.5	4.2	6.9	7.6	6.2	7.4

[a]M_1 is based on changes in column weight; M_2 is based on alkalinity loss; M_3 is based on Ca loss; M_4 is based on destructive sampling.
[b]Calculated using the anomalous data of Figure 4. Believed to be an underestimate of the actual value.

Table 3
$CaCO_3$ Concentration in the Columns Receiving Bicarbonate Solution Based on Destructive Sampling and Acid Digestion

Distance from Inlet (cm)	$CaCO_3$ Column (mg/g iron)	TCE + $CaCO_3$ (mg/g iron)
0.0 to 2.0	26.6	24.6
4.0 to 6.0	30.8	34.3
8.0 to 10.0	30.5	26.2

amount of precipitate (greater porosity loss) in the TCE + carbonate column may have been a consequence of greater corrosion of the iron through TCE reduction and thus greater OH^- production. Of particular note, precipitates formed to some maximum value over the entire length of each column, and in all cases, the precipitated $CaCO_3$ represented less than 10% of the initial porosity.

A significant objective of the study was to determine the effect of precipitate formation on hydraulic conductivity. This objective was compromised to a degree by the scatter in the hydraulic conductivity data (Figure 3). There is no apparent reason for the large increase in hydraulic conductivity in the TCE + $CaCO_3$ column between ~ 500 and 700 PV, nor is there any apparent reason for the decline in conductivity in the $CaCO_3$ column at ~ 200 PV. In spite of the uncertain quality of these data, it is reasonable to conclude that the loss in porosity caused by precipitate formation did not cause a substantial reduction in hydraulic conductivity, and indeed there is no apparent trend in hydraulic conductivity over the period of precipitate formation. Furthermore, because precipitate formation had substantially slowed and perhaps halted by 1000 PV, there is no reason to expect that precipitation of $CaCO_3$ would have a significant effect on hydraulic conductivity in the future.

As noted previously, in the early stage when gas accumulated to ~ 10% of the initial porosity, there was a decline in hydraulic conductivity of about one order of magnitude. However, the accumulation of precipitates to ~ 6% of the initial porosity had no substantial effect on hydraulic conductivity. Because the gas phase is the non-wetting fluid, it accumulates in the largest pores—those that are most effective in transmitting water. Precipitates on the other hand are likely to form as patches on the iron surface, in response to variation in local pH values, rather than being influenced by pore size. Using the measured specific surface area of the iron, an accumulation of ~ 30 mg/g, as observed in this study, and if a uniform layer of precipitate is assumed, the thickness of the layer would be 0.01 μm. This would be small relative to the diameters of most pores and would therefore not be expected to have a major influence on hydraulic conductivity.

Process and Progress of Precipitate Formation

Considering both columns that received carbonate and considering the entire columns, the evidence of the previous section indicates accumulation of $CaCO_3$ to a value of ~ 30 mg/g of iron, representing ~ 7 % of the initial porosity, followed by no further accumulation. It is not clear, however, if this occurred uniformly with time over the entire iron bed or if it occurred as a moving front of precipitate accumulation. Figure 5a shows profiles of relative alkalinity at various times for the TCE + $CaCO_3$ column (a comparable graph for the $CaCO_3$ column was similar and is therefore not shown). At early time (280 PV), almost the entire decline in bicarbonate occurred within the first 5 cm of the column, indicating this to be the primary region of precipitate formation. At later time (630 PV), the rate of loss in the first 2 to 5 cm declined while the rate of loss toward the effluent end increased. By 2500 PV, there was essentially no loss of bicarbonate over the entire length of the column. Thus, even over the short length of the columns used in this study (10 cm) and at the relatively high velocities (85 cm/d), there is evidence that $CaCO_3$ precipitated as a moving front through the column. That is, once $CaCO_3$ accumulated to ~ 30 mg/g of iron (~ 7% of the initial porosity), there was no further precipitation and the Ca and HCO_3^- continued farther into the column where conditions

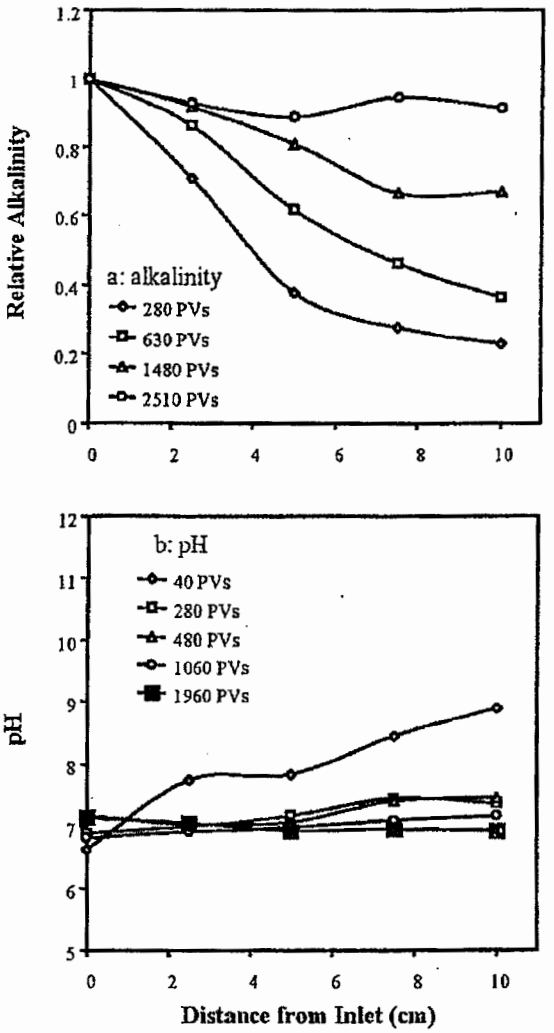

Figure 5. Changes in alkalinity and pH over time in the TCE + $CaCO_3$ column.

continued to be suitable for precipitate formation. As further evidence, Figure 5b shows pH profiles at various times for the TCE + $CaCO_3$ column. At early time (40 PV), the pH increased from an influent value of 6.8 to 7.8 by the first sampling port and 8.9 in the effluent. At 480 PV there was a slight increase in pH toward the effluent end while by 1060 PV, the pH was almost constant across the column. Corrosive production of OH^- and consumption through carbonate precipitation and formation of oxyhydoxide surface films influence pH. At early time, the increase in pH, followed by the plateau between 2.5 and 5 cm, is consistent with these competing processes, while the increase in pH toward the effluent end suggests the lack of carbonate precipitation in this region. This is consistent with the early time bicarbonate profile of Figure 5a. At late time, the pH is near neutral throughout the column and there is also little or no consumption of OH^- through carbonate precipitation. This implies little or no OH^- production along the column and thus greatly reduced corrosion rates.

It follows that the accumulation of $CaCO_3$ to values on the order of 30 mg/g iron has a passivating effect on the iron, greatly reducing the corrosion rates. As the corrosion rate declines, OH^- is not produced and thus $CaCO_3$ does not precipitate. The bicarbonate thus moves farther into the column until it reaches a zone where $CaCO_3$ has not precipitated to a level sufficient to passivate the iron, and thus OH^- production in this zone results in further precipitation of $CaCO_3$. Further evidence in support of this model is given in the following section.

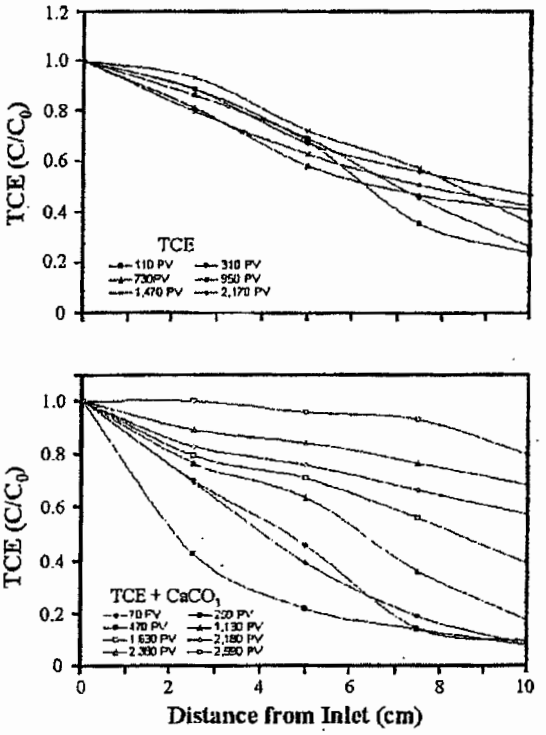

Figure 6. Changes in TCE concentration profiles in TCE and TCE + $CaCO_3$ columns.

TCE Degradation in the Presence of Bicarbonate

Figure 6 shows TCE concentration profiles at various times for the columns receiving TCE and TCE + $CaCO_3$. At early time, both columns showed degradation that was consistent with pseudo-first-order kinetics. The first-order rate-constant for the column receiving carbonate solution (k = 0.017/min) was, however, significantly greater than for that receiving only TCE (k = 0.0062/min). The reason for the difference in initial rate was not investigated but, as referred to previously, is most likely a consequence of enhanced corrosion caused by the bicarbonate ion. Of particular importance, while there was variation in the measured degradation profiles for the TCE column, there was no consistent trend over time, and the degradation rate at the conclusion of the experiment (k = 0.0045/min at 2170 PV) was similar to the initial value. In contrast, degradation in the TCE + $CaCO_3$ column departed from first-order behavior and showed a consistent decrease in degradation rate over time. Clearly, the accumulation of calcium carbonate caused a reduction in the rate of TCE degradation. Also, the rate of degradation declined most rapidly at early time near the influent end of the column, while the rate beyond the 5 cm point in the column was similar to the initial rate (note the graphs for 470 and 1130 PV). At later time (beyond ~ 2000 PV, the rates appear to be consistent with zero order kinetics, with the rate continuing to decline over time. By the end of the test (2590 PV), there was little degradation of TCE in the TCE + $CaCO_3$ column. This provides further evidence that the $CaCO_3$ precipitates have a passivating effect on the iron, and also that the precipitates form as a front moving through the column. It is perhaps noteworthy that while the maximum amount of precipitation had occurred by ~ 1500 PV, measurable degradation occurred beyond this time.

Implications

This study was conducted using short columns and flow velocities that were much higher than normally encountered under field conditions. Direct application of the results to field conditions must therefore be undertaken with a considerable degree of caution. Nevertheless, several of the observations and conclusions have direct relevance to the design of field installations.

Initial gas accumulations were on the order of 10% of the initial porosity, and resulted in declines in hydraulic conductivity of about one order of magnitude. Once the bubbling pressure of the iron bed was exceeded, the hydraulic conductivity recovered, but not to the initial values. Thus the design of installations should anticipate that the hydraulic conductivity of the PRB will be less, perhaps by a factor of three or four, than the saturated iron values. Furthermore, if the gas is not permitted to escape, declines of greater than one order of magnitude should be anticipated. This could be avoided through the installation of vent wells within the PRB.

Of particular importance is the observation that precipitates form to some maximum value, and that formation appears to occur as a diffuse front moving in the direction of flow through the PRB. Furthermore, the degree of

precipitation (~ 7% of the initial porosity) did not appear to have a measurable effect on hydraulic conductivity. Thus, where carbonate minerals are the primary precipitate, it does not appear that they will form to the point where the PRB will become impermeable. Thus, flushing solutions for removal of precipitates remains a potential maintenance option, as does the installation of a second parallel wall. The results also indicate that carbonate precipitates will passivate the iron, and that this zone of reduced activity will migrate over time from the influent surface into the PRB. Indeed, precipitate formation appears to be a self-regulating process, with the precipitates causing reduced reactivity which in turn reduces the rate of precipitate formation. To evaluate this phenomenon more fully, laboratory experiments that simulate field conditions more closely need to be conducted and careful monitoring and sectioning of PRBs that are already installed should be undertaken. Nevertheless, the results of this study suggest progressive passivation, and this should be considered in design. Design considerations could include added thickness or maintenance to periodically restore the activity of the iron.

As an example, and assuming the results of this study to be applicable to field conditions, we will assume that calcium carbonate accumulates to a maximum of 30 mg/g of iron. We will further assume a ground water velocity of 5 cm/d, an aquifer porosity of 0.3, a bicarbonate concentration of 100 mg/L, an iron bulk density of 3 g/cm^3 in the PRB, and that all of the bicarbonate is lost through precipitation as calcite. In reality, precipitation will occur across a diffuse front, with the width of the front dependent on several factors including initial concentration of bicarbonate, ground water velocity, and reaction rates. For the purpose of this calculation, it will be assumed that precipitation occurs at a sharp front. Under these conditions, the precipitate front would advance at a rate of ~ 1.0 cm/yr. Clearly, the rate of advance would be strongly dependent on the velocity and composition of the ground water, but under the assumed conditions, ~ 10 cm of a PRB could become nonreactive with respect to degradation of organic contaminants over a 10 yr period.

It should also be noted that reactive transport models (Yabusaki et al. 2001; Mayer et al. 2001) that have been applied to iron PRBs generally consider the reactivity of the iron to be constant over time. Thus, there is no upper limit on the amount of precipitate that could form and thus, given sufficient time, precipitation would continue until the initial void space was completely filled. It appears that if these models are to become useful for predicting long-term performance, the effect of precipitates on corrosion rate needs to be incorporated. Thus the relationship between the amount of precipitate present and iron reactivity should be quantified with greater precision.

Acknowledgements

The authors are grateful to Greg Friday and Wayne Noble for their expert and willing assistance in conducting the laboratory tests. We also appreciate the constructive comments of Drs. Gui and Odziemkowski on early drafts of the manuscript. Financial support for the study was provided through the Natural Sciences and Engineering Research Council-Motorola-EnviroMetal Industrial Research Chair held by Dr. Gillham.

References

Agrawal, A., W.J. Ferguson, B.O. Gardner, J.A. Christ, J.Z. Bandstra, and P.G. Tratnyek. 2002. Effects of carbonate species on the kinetics of dechlorination of 1,1,1-trichloroethane by zero-valent iron. *Environmental Science & Technology* 36, no. 20: 4326–4333.

Blowes, D.W., C.I. Ptacek, and J.L. Jamber. 1997. In-situ remediation of chromate contaminated groundwater using permeable reactive walls: Laboratory studies. *Environmental Science & Technology* 31, no. 12: 3348–3357.

Bonin, P.M.L., M.S. Odziemkowski, E.J. Reardon, and R.W. Gillham. 2000. In situ identification of carbonate-containing green rust on iron electrodes in solutions simulating groundwater. *Journal of Solution Chemistry* 29, no. 10: 1061–1074.

Bundy, L.G., and J.M. Bremner. 1972. A simple titrimetric method for determination of inorganic carbon in soils. *Soil Science Society of America Proceedings* 36 no. 2: 273–275.

Dahmke, M.E., R. Kober, and D. Schafer. 2000. Laboratory and field results of Fe(0) reaction walls—A first resume. In *Groundwater 2000*, ed. P.L. Bjerg, P. Engesgaard, and Th.D. Krom, 526. Rotterdam, Netherlands: A.A. Balkema.

Farrell, J., M. Kason, N. Melitas, and T. Li . 2000. Investigation of the long-term performance of zero-valent iron for reductive dechlorination of trichloroethylene. *Environmental Science & Technology* 34, no. 3: 514–521.

Fort, J.R. 2000. Physical performance of granular iron reactive barrier under aerobic and anoxic conditions. M.Sc. thesis, Department of Civil and Environmental Engineering, University of Wisconsin, Madison.

Fryar, A.E., and F.W. Schwartz. 1998. Hydraulic-conductivity reduction, reaction-front propagation, and preferential flow within a model reactive barrier. *Contaminant Hydrology* 32, 333–351.

Gallant, W.A., and B. Myller. 1997. The results of a zero-valent metal reactive wall demonstration at Lowry AFB, Colorado. In *Air and Waste Management Association's Annual Meeting and Exhibition*, Toronto, Ontario, Canada. June 8–13, p. 21.

Gillham, R.W. 1999. In situ remediation of VOC-contaminated groundwater using zero-valent iron: Long-term performance. In *The 1999 Contaminated Site Remediation Conference "Challenges Posed by Urban & Industrial Contaminants"* organized by The Centre for Groundwater Studies, Fremantle, Western Australia, March 21–25, pp. 605–614.

Gillham, R.W., and S.F. O'Hannesin. 1994. Enhanced degradation of halogenated aliphatics by zero-valent iron. *Ground Water* 32, no. 6: 958–967.

Klausen, J., P.J. Vikesland, T. Kohn, R. Burris, W.P. Ball, and A.L. Roberts. 2003. Longevity of granular iron in groundwater treatment processes: Solution composition effects on reduction of organohalides and nitroaromatic compounds. *Environmental Science & Technology* 37, no. 6: 1208–1218.

Mackenzie, P.D., D.P. Horney, and T.M. Sivavec. 1999. Mineral precipitation and porosity losses in granular iron columns. *Journal of Hazardous Materials* 68, no. 1–2: 1–17.

Matheson, L.J., and P.G. Tratnyek. 1994. Processes affecting remediation of contaminated groundwater by dehalogentain with iron. *Environmental Science & Technology* 28, no. 12: 2045–2052.

Mayer, K.U., D.W. Blowes, and E.O. Frind. 2001. Reactive transport modeling of an in situ reactive barrier for the treatment of hexavalent chromium and trichloroethylene in groundwater. *Water Resources Research* 37, no. 12: 3091–3103.

McMahon, P.B., K.F. Denneky, and M.W. Sandstrom. 1999. Hydraulic and geochemical performance of a permeable

reactive barrier containing zero-valent iron, Denver Federal Centre. *Ground Water* 37, no. 3: 396–404.

Morrison, S.J., R.R. Spangler, and S.A. Morris. 1996. Subsurface injection of dissolved ferric chloride to form a chemical barrier: Laboratory investigations. *Ground Water* 28, no. 1: 75–83.

O'Hannesin, S.F., and R.W. Gillham. 1998. Long-term performance of an in situ "iron wall" for remediation of VOCs. *Ground Water* 36, no. 1: 164–170.

Okwi, G., N.R. Thomson, and R.W. Gillham. In press. The impact of permanganate on the ability of granular iron to degrade trichloroethene. *Ground Water Monitoring & Remediation.*

Phillips, D.H., B. Gu, D.B. Watson, Y. Roh, L. Liang, and S.Y. Lee. 2000. Performance evaluation of a zero valent iron reactive barrier: Mineralogical characteristics. *Environmental Science & Technology* 34, no. 18: 4167–4176.

Reardon, E.J. 1995. Anaerobic corrosion of granular iron: Measurement and interpretation of hydrogen evolution rates. *Environmental Science & Technology* 29, no. 12: 2936–2945.

Repta, C.J.W. 2001. Evaluation of nickel-enhanced granular iron for the dechlorination of trichlorethene. M.Sc. thesis, Department of Earth Sciences, University of Waterloo, Waterloo, Ontario.

Reynolds, T.J. 2002. An evaluation of the ten-year performance of a permeable reactive barrier including an assessment of the in situ microcosm technique. M.Sc. thesis, Department of Earth Sciences, University of Waterloo, Waterloo, Ontario.

Ritter, K., M.S. Odziemkowski, and R.W. Gillham. 2002. An in situ study of the role of surface films on granular iron in the permeable iron wall technology. *Journal of Contaminant Hydrology* 55, 87–111.

Sorel, D., S.D. Warner, B.L. Longino, J.H. Honniball, and L.A. Hamilton. 2003. Performance monitoring and dissolved hydrogen measurements at a permeable zero valent iron reactive barrier. In *Chlorinated Solvent and DNAPL Remediation, Innovative Strategies for Subsurface Cleanup, ACS Symposium Series* 837, ed. S.M. Henry and S.D. Warner, 259–277.

Vogan, J.L., R.M. Focht, D.K. Clark, and S.L. Graham. 1999. Performance evaluation of a permeable reactive barrier for remediation of dissolved chlorinated solvents in groundwater. *Journal of Hazardous Material* 68, no. 1–2: 97–108.

Yabusaki, S., K. Cantrell, B. Sass, and S. Carl. 2001. Multicomponent reactive transport in an in situ zero-valent iron cell. *Environmental Science & Technology* 35, no. 7: 1493–1503.